GENOMICS AND COMPUTATIONAL BIOLOGY Vol. 3 No. 1 (2017): e53

Short Communication

Development of 3D Tissue Reconstruction Method from Single-cell RNA-seq Data

Tomoya Mori[1], Junko Yamane[1], Kenta Kobayashi[1], Nobuko Taniyama[1], Takanori Tano[2], Wataru Fujibuchi[1,*]

[1]Center for iPS Cell Research and Application, Kyoto University, 53 Kawahara-cho, Sakyo-ku, Kyoto, 606-8507 Japan
[2]Biomedical Research Department, Ricoh Institute of Future Technology, Ricoh Company, Ltd., 16-1 Shinei-cho, Tsuzuki-ku, Yokohama, Kanagawa, 224-0035 Japan

*Correspondence: Tel: +81 75 366 7012; Fax: +81 75 366 7013; Email: fujibuchi-g@cira.kyoto-u.ac.jp

Received 2016-10-11; Accepted 2016-11-02

SUMMARY

In silico three-dimensional (3D) reconstruction of tissues/organs based on single-cell profiles is required to comprehensively understand how individual cells are organized in actual tissues/organs. Although several tissue reconstruction methods have been developed, they are still insufficient to map cells on the original tissues in terms of both scale and quality. In this study, we aim to develop a novel informatics approach which can reconstruct whole and various tissues/organs *in silico*. As the first step of this project, we conducted single-cell transcriptome analysis of 38 individual cells obtained from two mouse blastocysts (E3.5d) and tried to reconstruct blastocyst structures in 3D. In reconstruction step, each cell position is estimated by 3D principal component analysis and expression profiles of cell adhesion genes as well as other marker genes. In addition, we also proposed a reconstruction method without using marker gene information. The resulting reconstructed blastocyst structures implied an indirect relationship between the genes of Myh9 and Oct4.

INTRODUCTION

Three-dimensional (3D) tissue construction from induced pluripotent stem (iPS)-derived cells using cell sheet technology and/or 3D bioprinting systems is one of the most attractive approaches in regenerative medicine. However, to generate artificial and functional tissues/organs in 3D manner is still challenging due to their structural complexity. Recently, the single-cell analysis technology has evolved to obtain cell profiles at much higher resolution than ever before, which enables us to investigate cellular heterogeneity in such complex tissues/organs in more details [1–3]. To date, several computational methods to reconstruct tissues from single-cell gene expression data have been reported. Durruthy-Durruthy et al. analyzed 382 individual mouse otocyst and neuroblast cells and reconstructed a mouse otocyst structure by 3D principal component analysis (PCA) [4]. This method was also applied to early and late human blastocysts in [5]. However, each cell was mapped to only the surface of a sphere and it was still insufficient to map cells on the original tissue structure. On the other hand, Satija et al. used 851 single-cells dissociated from zebrafish embryos and inferred their spatial positions by combining gene expression patterns and *in situ* hybridization patterns obtained from a database [6]. Similarly, Achim et al. also proposed another *in situ* hybridization based reconstruction method and applied it to 213 single-cell RNA-seq data of a developing brain of a marine annelid (*P. dumerilii*) [7]. Nevertheless, both approaches require *in situ* hybridization data as a reference map for accurate mapping of cells, which limits applicability of the approaches.

In this study, we aim to develop an *in silico* 3D tissue reconstruction method which can be applied to whole and various tissues/organs. As the first step of the project, we reconstruct blastocyst structures based on single-cell transcriptome data obtained from mouse blastocysts. The main contributions of this study are as follows. (i) We obtain at least 18 cells from a blastocyst (E3.5d) in contrast to average 8 cells from a blastocyst (E5.0d - E6.0d) in [5] towards an *in silico* 3D tissue reconstruction from one individual tissue transcriptome data. (ii) We propose an *in silico* reconstruction method which can map cells not only to the surface but also to the inner side of a sphere structure by referring expression levels of known marker genes. (iii) We also develop another reconstruction method without using marker gene information.

RESULTS

Cell dissociation and sequencing

We dissociated two mouse blastocysts (E3.5d) and obtained single-cell transcriptome of 38 individual cells, where 20 cells (Cell.1_1 - Cell.1_20) were from a blastocyst cultured for 0 hour (Blastocyst 1) and 18 cells (Cell.2_1 - Cell.2_18) were from the other blastocyst cultured for two hours (Blastocyst 2). Sample preparation was done by the following procedures: (i) weaken cell adhesion in the blastocysts by trypsinization after removing the zona pellucida, (ii) dissociate the blastocysts into single-cells by mouth pipetting and collect them into cell lysis buffer containing barcode oligos with manual picking, (iii) incorporate the barcode sequences into the mRNAs by template switching method during reverse transcription, (iv) run sequencing and obtain single-cell transcriptome data using Illumina HiSeq 2500 after sequence library preparation.

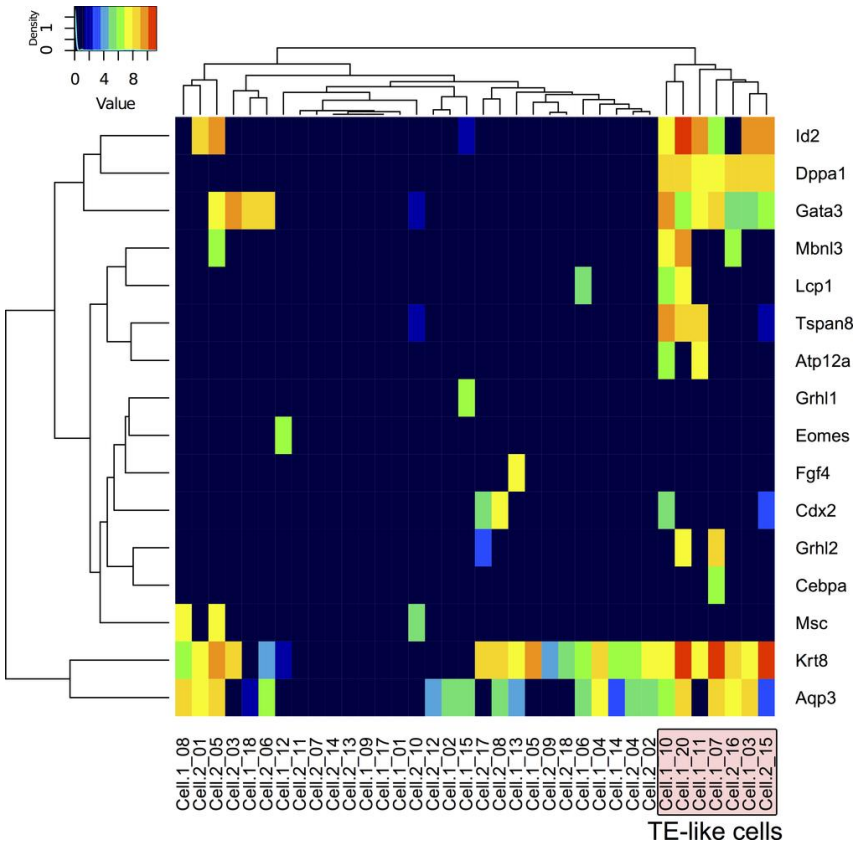

Figure 1: Heatmap of expression levels of TE marker genes.

Mapping of sequence reads

The resulting sequence reads were mapped to the mouse (C57BL/6J) genome sequence data downloaded from Ensembl database (GRCm38, release 85) [8]. We employed Bowtie2 [9] and HTSeq [10] as a mapping tool and a read counting tool, respectively. The total number of reads which passed quality control was 74,235,305, and the average mapping rate was 94.40%. However, we removed two cells from the 20 cells of Blastocyst 1 for the following data analysis and reconstruction procedures since the numbers of sequence reads of the two cells were quite small (around only 1,000).

Detecting trophectoderm-like cells

A blastocyst of E3.5d is mainly composed of trophectoderm (TE) and inner cell mass (ICM). Although cells of TE and ICM are located on the surface and inner side of the blastocyst structure respectively, their spatial information was lost during cell dissociation. In order to detect cell types of individual cells from the transcriptome data, we performed clustering analysis of the 36 cells according to expression levels of TE marker genes selected in [11]. The clustering result (Figure 1) shows that TE markers are relatively highly expressed in the seven cells (TE-like cells hereafter).

3D reconstruction of mouse blastocyst using marker gene information

Mapping of the 18 cells from Blastocyst 1 and 18 cells from Blastocyst 2 into a 3D space was done by 3D PCA based on gene expression levels of 46 marker genes of TE, ICM, primitive endoderm (PE), pluripotent epiblast (EPI) cells as well as 544 cell adhesion associated genes. Then, we generated sphere models by applying the whitening/sphering transformation employed in original 3D PCA-based reconstruction method [3]. Here, each cell is mapped only to the surface of the sphere. In order to map the cells not only to the surface but also to the inner side of the sphere, we adjusted distance from the center point of the sphere to each cell position according to average expression levels of TE marker genes (e.g., Cdx2, Gata3, and Id2) and ICM marker genes (e.g., Oct4 and Nanog) so that TE-like cells are mapped outer side while ICM-like cells are mapped inner side of the sphere. The resulting reconstructed blastocyst structures indicate that our proposed method generates a mouse blastocyst structure reflecting the different gene expression patterns between TE and ICM cells (Figure 2).

3D reconstruction of mouse blastocyst without using marker gene information

The 3D reconstruction method described above used the already known marker gene information (i.e., TE and

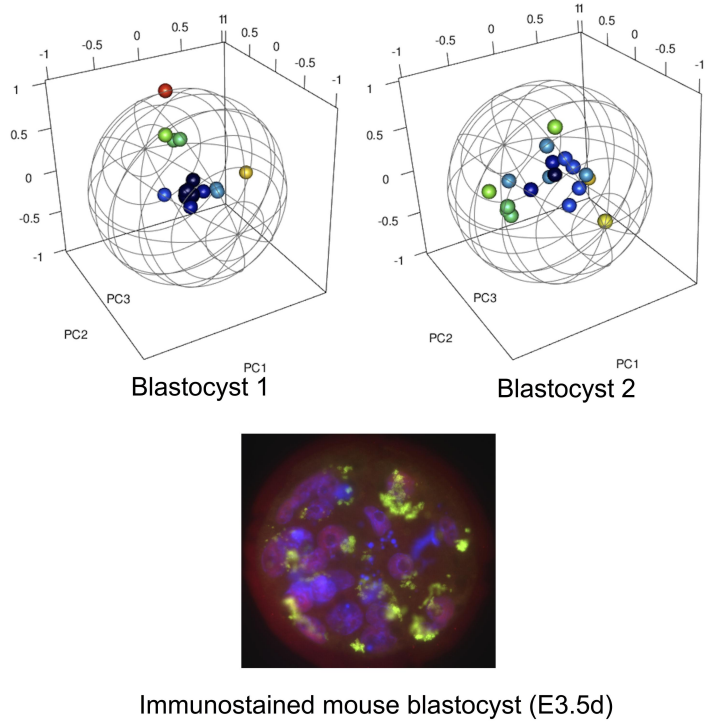

Figure 2: Reconstructed mouse blastocyst structures and an actual mouse blastocyst. Each point in the upper panels indicates individual cell. TE-like cells are colored red/yellow while ICM-like cells are colored green/blue. The bottom panel indicates immunostaining of Hoechst (blue), Cdx2 (red), and Oct3/4 (green).

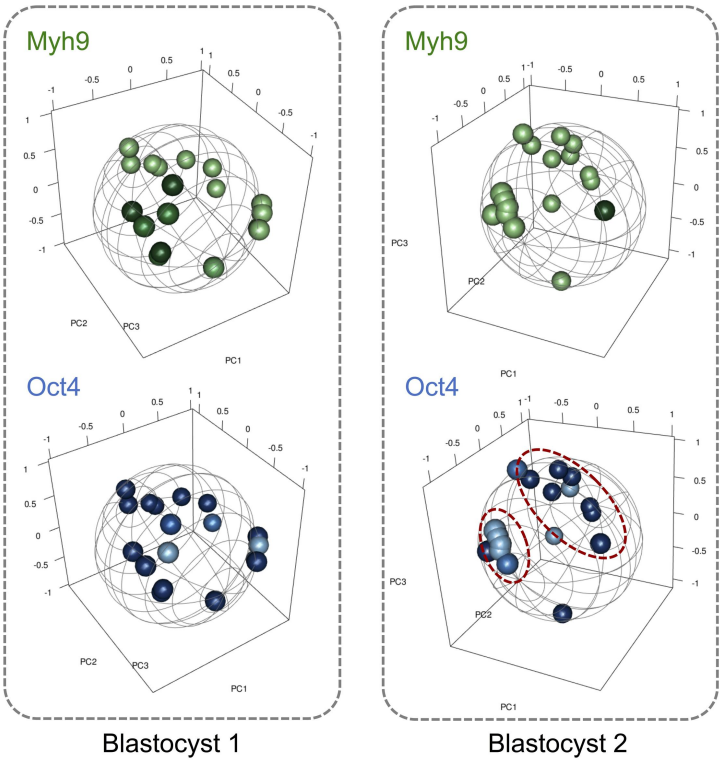

Figure 3: Reconstructed mouse blastocyst structures without using known marker gene information. Color strength indicates expression level of Myh9 (green) and Oct4 (blue). Dashed circles indicate expression domains in which cells have similar expression levels.

ICM marker genes). However, such marker information is not always available, so that development of a 3D reconstruction method without using marker genes information will be required for various tissues/organs reconstruction.

Thus, in order to reconstruct a blastocyst without using marker gene information, we focused on the non-muscle myosin heavy polypeptide 9 gene (Myh9) since Maître et al. reported that actomyosin contractility is deeply involved in cell positioning and fate decisions of blastomeres in mouse embryo by using a 3D physical model of embryo morphogenesis and Myh9-knockout chimaeric embryos [12]. We performed partial least squares (PLS) regression of Myh9 and selected the top 716 genes having high regression coefficients for Blastocyst 1 and Blastocyst 2 respectively, which are equivalent to 5% of the total number of expressed genes. After that, for Blastocyst 1 and Blastocyst 2, we generated sphere models based on 3D PCA using the 716 genes (Figure 3). The distances from the center of the sphere to cells were determined by expression levels of Myh9, and color strength indicates expression levels of Myh9 (green) and Oct4 (blue). In both cases of Blastocyst 1 and Blastocyst 2, cells having similar expression levels of Myh9 were mapped near each other. On the other hand, there was no correlation between the expressions of Oct4 and Myh9. However, in Blastocyst 2, we can see domains in which cells have similar expression levels of Oct4, although Oct4 is not included in the 716 genes. These results imply an indirect relationship between Myh9 and Oct4.

DISCUSSION

We developed an *in silico* 3D tissue reconstruction method based on PCA with/without marker gene expressions information. However, it is still not sufficient to reconstruct whole and various tissues. For further improvement of the method using marker gene information, to obtain accurate cell positions of specific cell types by immunostaining of marker proteins such as Oct3/4 and to use them as a reference map are needed. On the other hand, for the method without using marker information, to select more effective set of genes which may associate with controlling cell positioning and cell fate other than Myh9 such as actin and cytoskeleton associated genes is left as future work.

ACKNOWLEDGEMENTS

This study was partially supported by a collaborative research funding from Ricoh Company, iPS Cell Research Fund, the Future Development Funding Program of Kyoto University Research Coordination Alliance, and Core Center for iPS Cell Research, Research Center Network for Realization of Regenerative Medicine, Japan Agency for Medical Research and Development.

CONFLICT OF INTEREST

The authors declare no conflict of interest.

REFERENCES

1. Li J, Klughammer J, Farlik M, Penz T, Spittler A, Barbieux C, et al. **Single-cell transcriptomes reveal characteristic features of human pancreatic islet cell types.** EMBO reports. 2016;17(2):178–187. doi:10.15252/embr.201540946.
2. Zeisel A, Muñoz-Manchado AB, Codeluppi S, Lönnerberg P, La Manno G, Juréus A, et al. **Cell types in the mouse cortex and hippocampus revealed by single-cell RNA-seq**. Science. 2015;347(6226):1138–1142. doi:10.1126/science.aaa1934.
3. Grün D, Lyubimova A, Kester L, Wiebrands K, Basak O, Sasaki N, et al. **Single-cell messenger RNA sequencing reveals rare intestinal cell types**. Nature. 2015;525(7568):251–255. doi:10.1038/nature14966.
4. Durruthy-Durruthy R, Gottlieb A, Hartman BH, Waldhaus J, Laske RD, Altman R, et al. **Reconstruction of the mouse otocyst and early neuroblast lineage at single-cell resolution**. Cell. 2014;157(4):964–978. doi:10.1016/j.cell.2014.03.036.
5. Durruthy-Durruthy J, Wossidlo M, Pai S, Takahashi Y, Kang G, Omberg L, et al. **Spatiotemporal reconstruction of the human blastocyst by single-cell gene-expression analysis informs induction of naive pluripotency**. Developmental Cell. 2016;38(1):100–115. doi:10.1016/j.devcel.2016.06.014.
6. Satija R, Farrell JA, Gennert D, Schier AF, Regev A. **Spatial reconstruction of single-cell gene expression data**. Nature Biotechnology. 2015;33(5):495–502. doi:10.1038/nbt.3192.
7. Achim K, Pettit JB, Saraiva LR, Gavriouchkina D, Larsson T, Arendt D, et al. **High-throughput spatial mapping of single-cell RNA-seq data to tissue of origin**. Nature Biotechnology. 2015;33(5):503–509. doi:10.1038/nbt.3209.
8. Yates A, Akanni W, Amode MR, Barrell D, Billis K, Carvalho-Silva D, et al. **Ensembl 2016**. Nucleic Acids Research. 2016;44(D1):D710–D716. doi:10.1093/nar/gkv1157.
9. Langmead B, Salzberg SL. **Fast gapped-read alignment with Bowtie 2**. Nature Methods. 2012;9(4):357–359. doi:10.1038/nmeth.1923.
10. Anders S, Pyl PT, Huber W. **HTSeq - A Python framework to work with high-throughput sequencing data**. Bioinformatics. 2015;31(2):166–169. doi:10.1093/bioinformatics/btu638.
11. Guo G, Huss M, Tong GQ, Wang C, Sun LL, Clarke ND, et al. **Resolution of cell fate decisions revealed by single-cell gene expression analysis from zygote to blastocyst**. Developmental Cell. 2010;18(4):675–685. doi:10.1016/j.devcel.2010.02.012.
12. Maître JL, Turlier H, Illukkumbura R, Eismann B, Niwayama R, Nédélec F, et al. **Asymmetric division of contractile domains couples cell positioning and fate specification.** Nature. 2016;536(7616):344–348. doi:10.1038/nature18958.

Supplementary file:

53_Mori_HighRes_Figure1.jpg

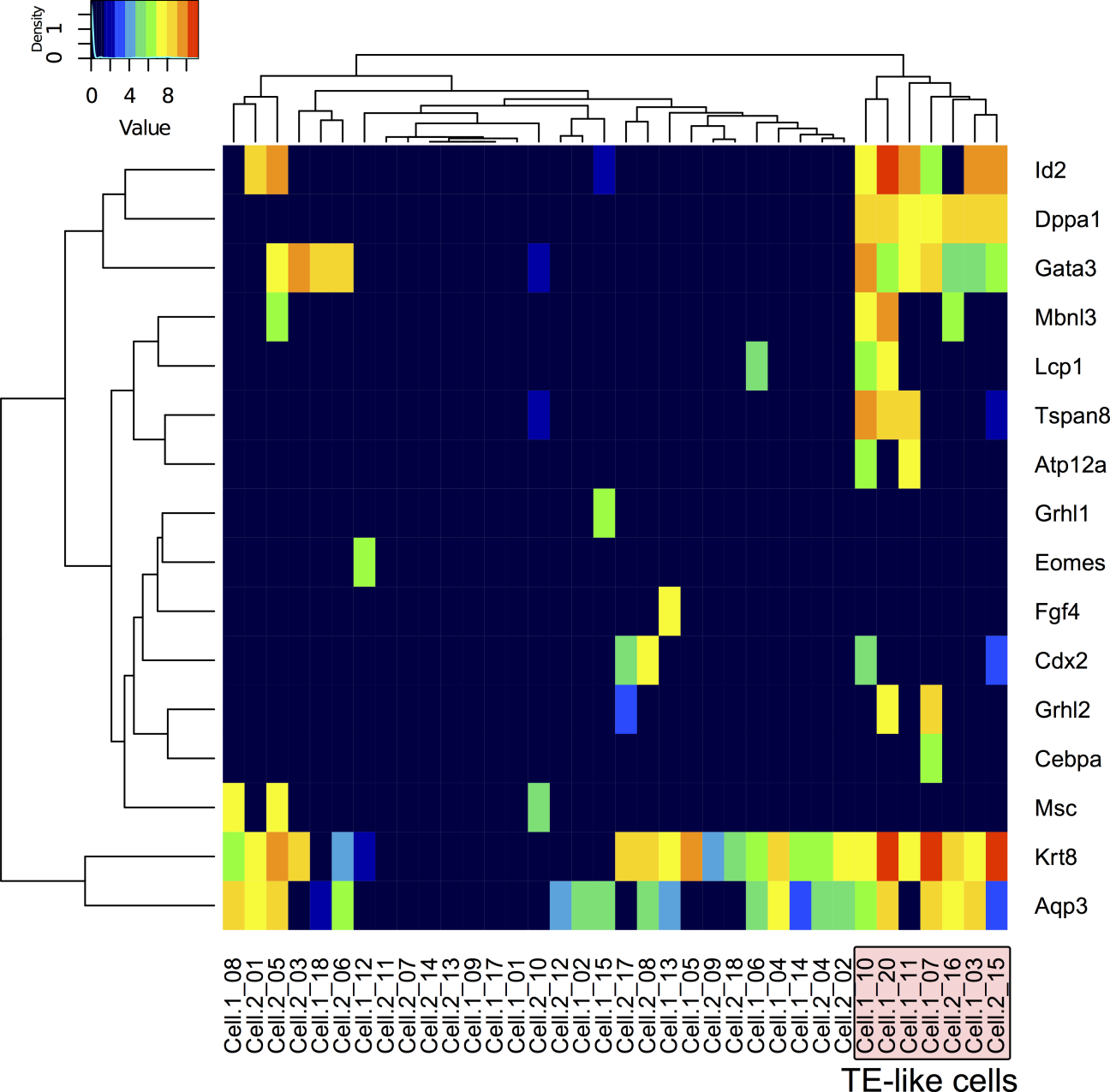
Density
0
1
0
4
8
Value
Id2
Dppa1
Gata3
Mbnl3
Lcp1
Tspan8
Atp12a
Grhl1
Eomes
Fgf4
Cdx2
Grhl2
Cebpa
Msc
Krt8
Aqp3
Cell.1_08
Cell.2_01
Cell.2_05
Cell.2_03
Cell.1_18
Cell.2_06
Cell.1_12
Cell.2_11
Cell.2_07
Cell.2_14
Cell.2_13
Cell.1_09
Cell.1_17
Cell.1_01
Cell.2_10
Cell.2_12
Cell.1_02
Cell.1_15
Cell.2_17
Cell.2_08
Cell.1_13
Cell.1_05
Cell.2_09
Cell.2_18
Cell.1_06
Cell.1_04
Cell.1_14
Cell.2_04
Cell.2_02
Cell.1_10
Cell.1_20
Cell.1_11
Cell.1_07
Cell.2_16
Cell.1_03
Cell.2_15
TE-like cells

Supplementary file:

53_Mori_HighRes_Figure2.jpg

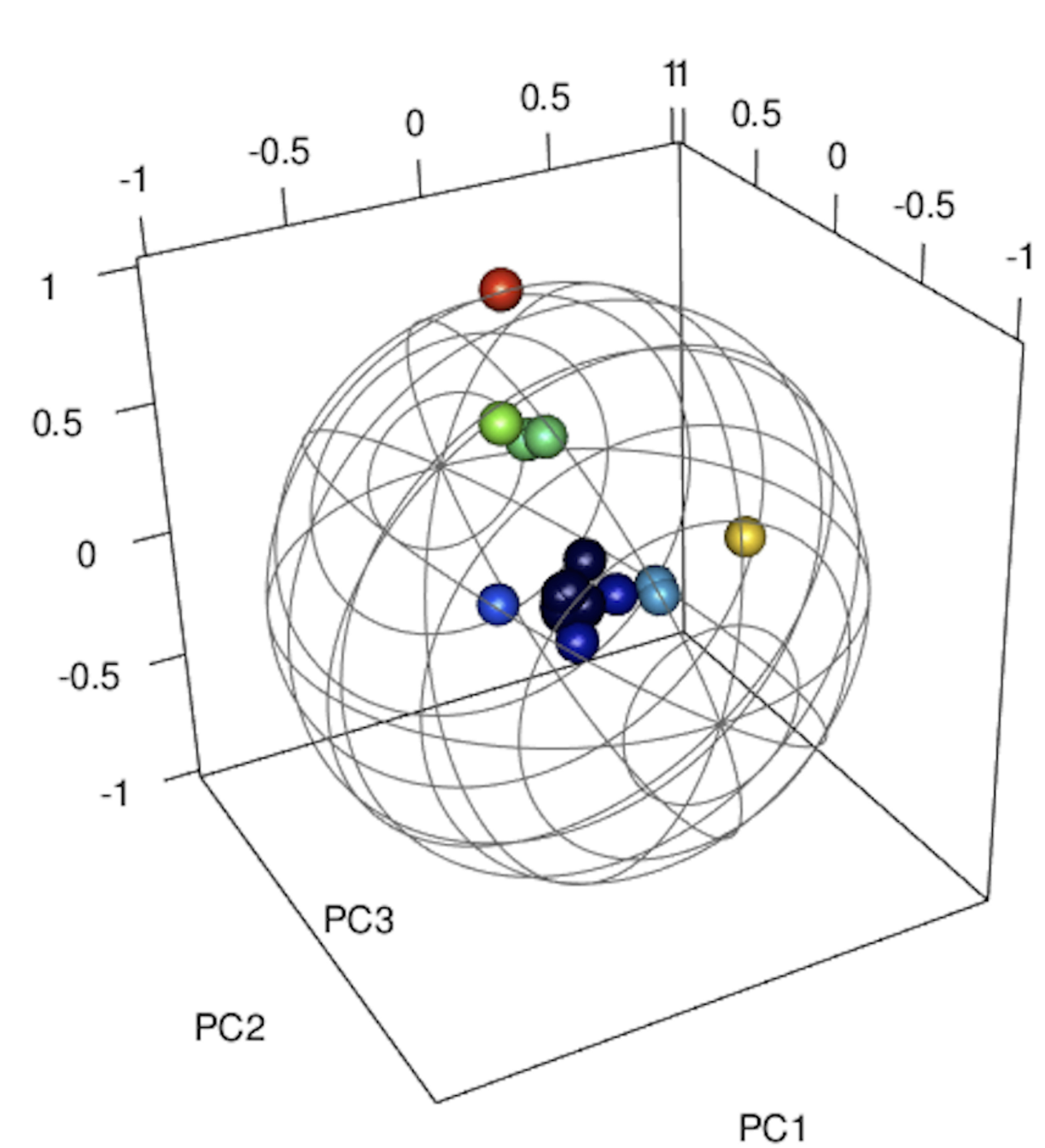

Blastocyst 1

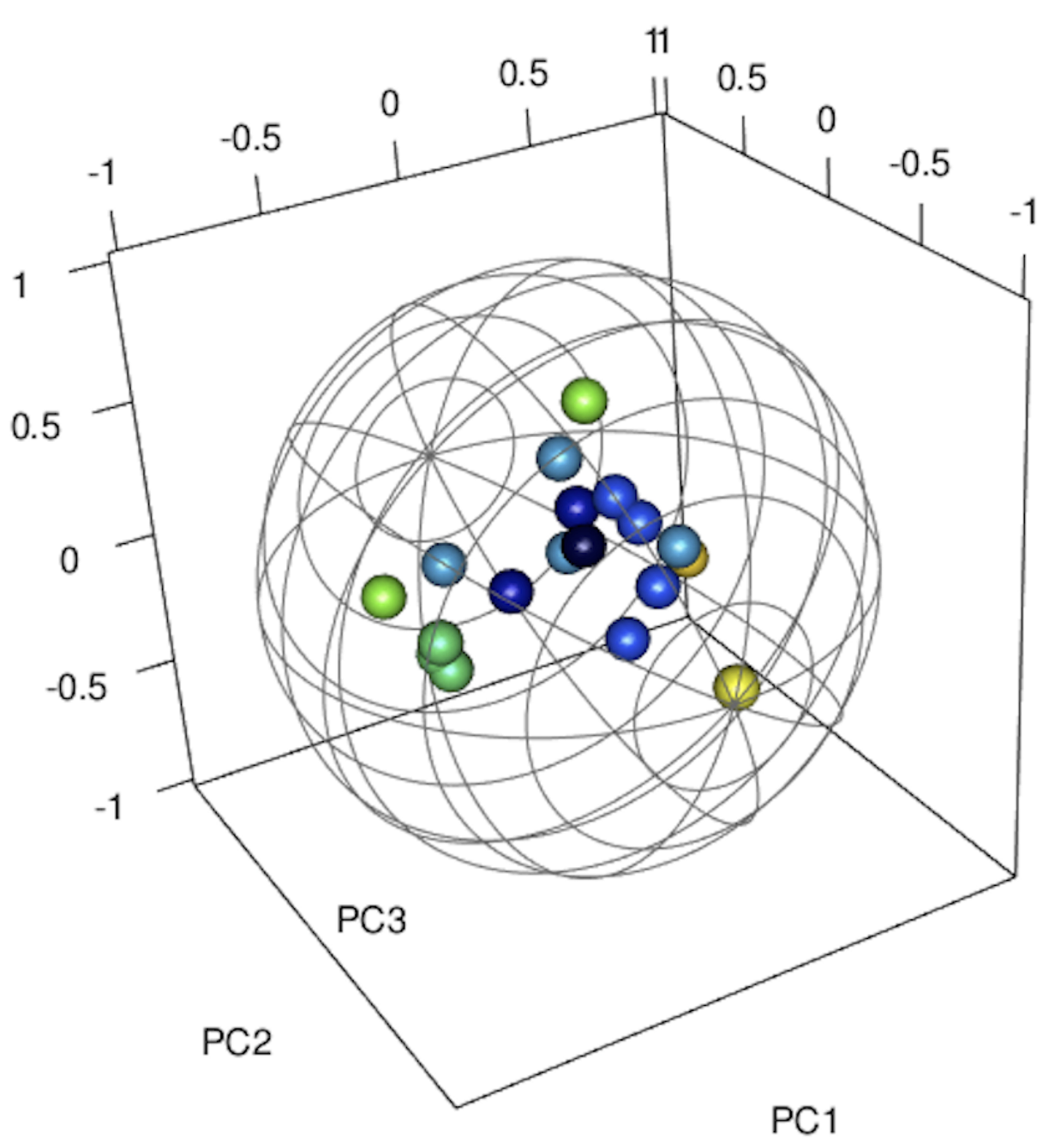

Blastocyst 2

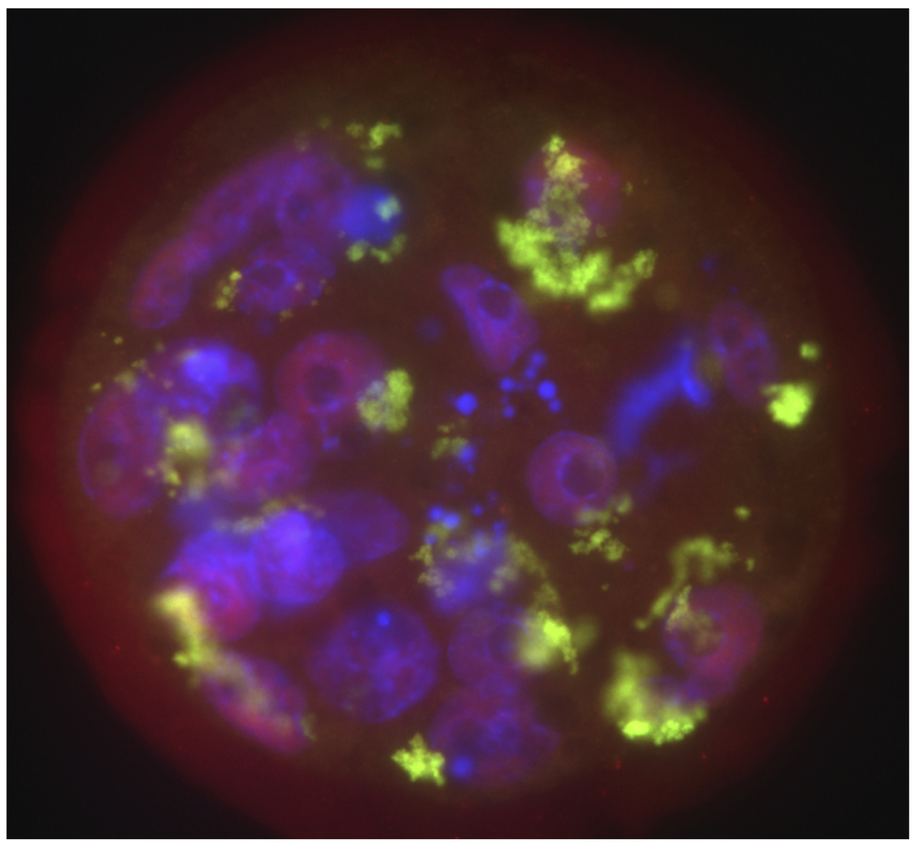

Immunostained mouse blastocyst (E3.5d)

Supplementary file:

53_Mori_HighRes_Figure3.jpg

Myh9

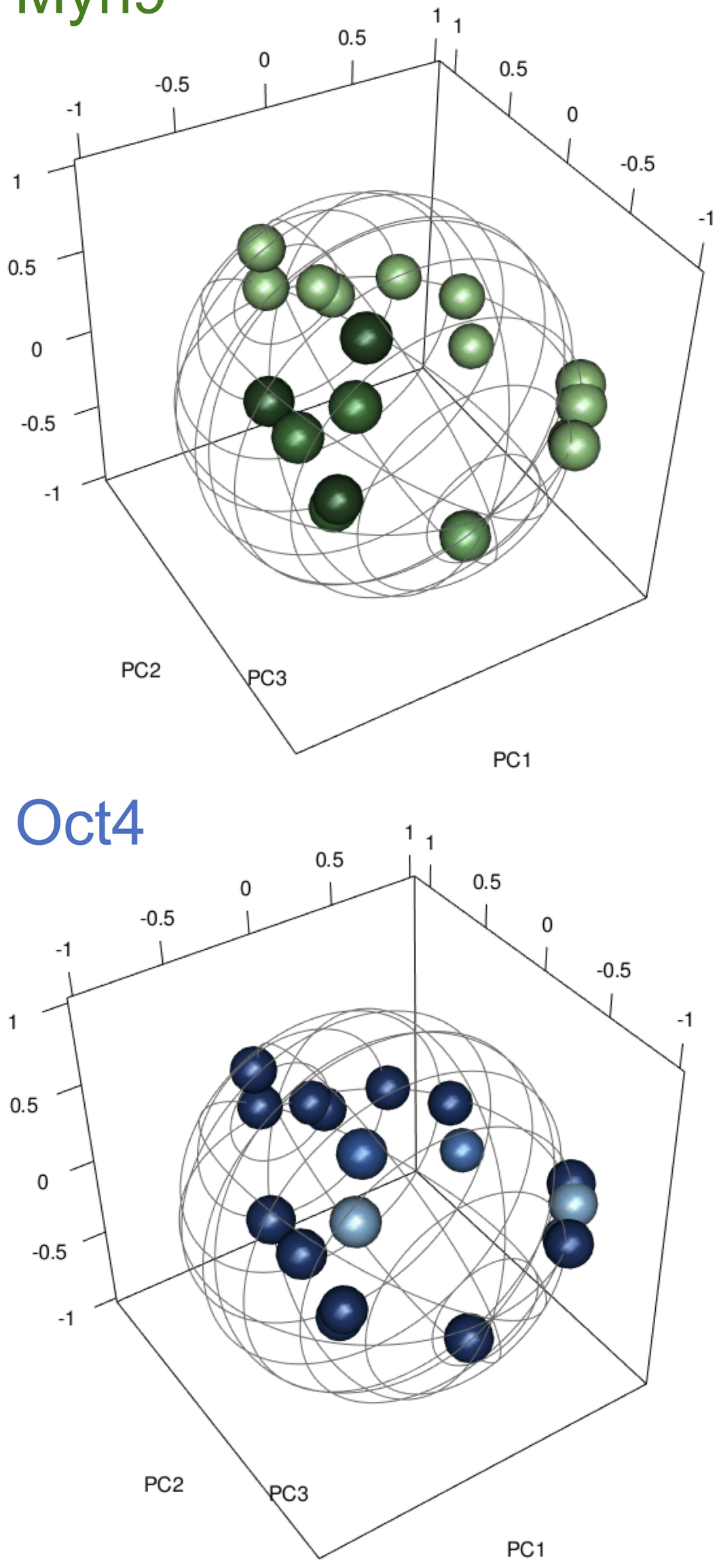

Myh9

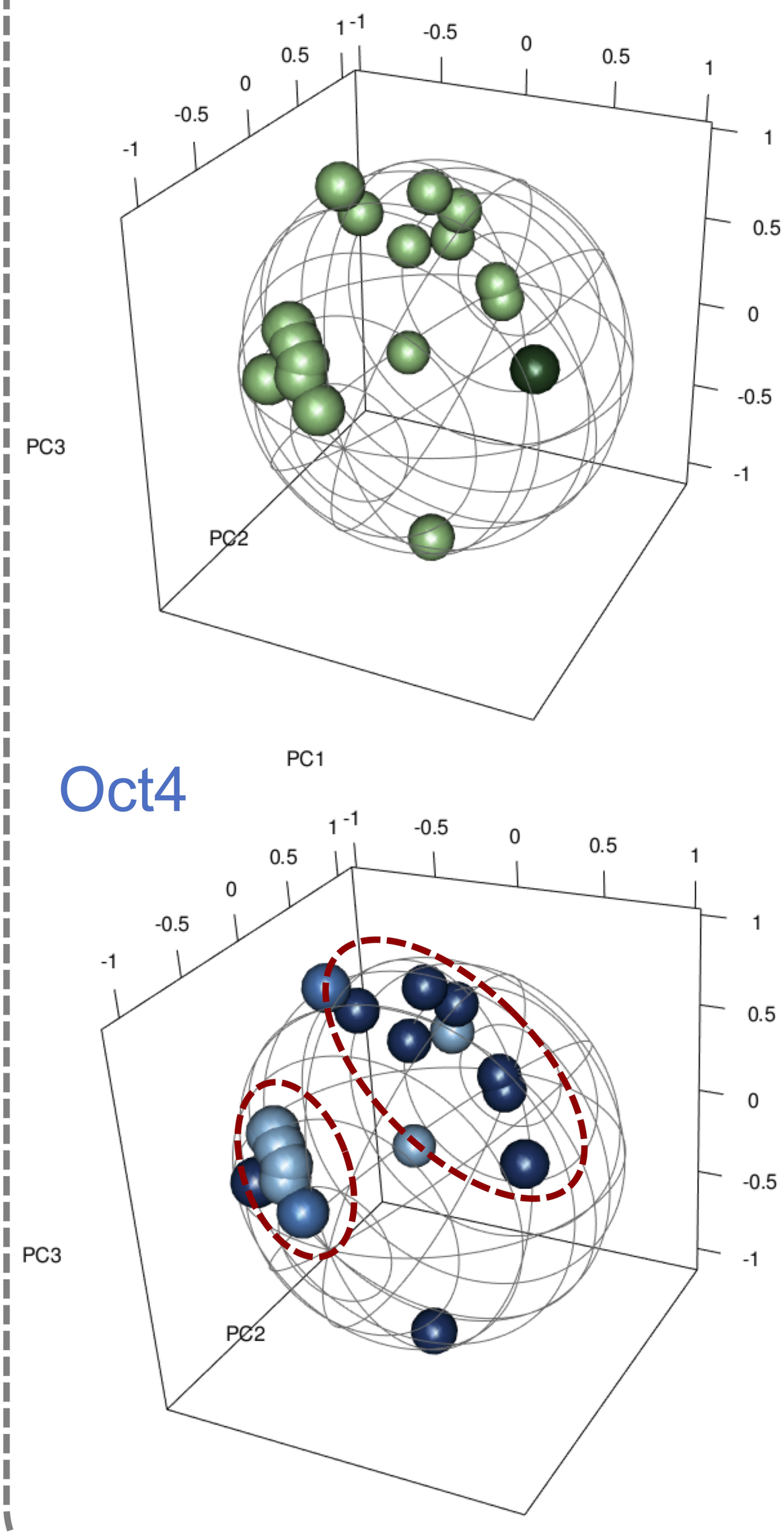

Oct4

Oct4

Blastocyst 1

Blastocyst 2